PREDICTING MOVABLE BED ROUGHNESS IN COASTAL WATERS

Chelsea Joy Humbyrd[1] and Ole Secher Madsen[2]

Accurately predicting movable bed roughness is essential to the analyses of transport processes, but when the bottom is rippled, as it commonly is in the coastal environment, characterizing the roughness is less straightforward than when the bottom is flat. The common method of predicting roughness, while effective, unnecessarily predicts ripple geometry and requires a model-dependent factor, which varies widely, relating ripple geometry and bottom roughness. We have therefore developed an alternative, more direct method of predicting bed roughness in the ripple regime: the wave energy dissipation factor is predicted from flow and sediment information and then any desired theoretical friction factor model is used to back-calculate the roughness. This paper describes the common and proposed methods of predicting roughness and presents results of preliminary testing of the methods with field data. Both methods adequately predict current velocities in wave-current field flows, with the proposed method yielding the smaller RMS-error of 3.1 cm/s. Remaining questions concerning the appropriate near-bottom orbital velocity required to describe field conditions must be resolved when additional field data becomes available.

Keywords: movable bed roughness; ripple geometry; wave energy dissipation; wave-current interaction

INTRODUCTION

Accurately predicting transport processes, including sediment transport, in the coastal environment is impossible without correct current velocity and shear stress information. An estimate of the movable bed roughness is necessary to predict these quantities, and while this roughness is scaled by the sand grain diameter for flat beds, in the coastal environment where wave-generated ripples commonly cover the bed, the roughness is scaled by the ripple dimensions. In the ripple regime, therefore, the roughness is often naturally taken as a function of the ripple geometry, which is predicted from fluid, flow, and sediment parameters. Finding the roughness with this method, however, requires a constant that depends on the choice of theoretical friction factor model.

Instead of first predicting the ripple dimensions, which are not otherwise needed, we propose to directly predict the wave energy dissipation factor, which can be obtained experimentally and is not model-dependent. Any model can then be used to back-calculate the bed roughness. In this paper we discuss the details of this proposed method, developed using laboratory data, and the results of testing the two methods with data from combined wave-current flows in the field.

METHODS OF PREDICTING ROUGHNESS

Energy dissipation

When wave attenuation is measured in laboratory experiments, the wave energy dissipation factor, f_e, can be directly calculated from energy conservation considerations. The time-averaged rate of energy dissipation per unit area, $\dot{E}_{diss}$, can be calculated based on linear wave theory from the measured wave height decay over the length of the flume by

$$\dot{E}_{diss} = \rho g c_g a \left|\frac{da}{dx}\right| \tag{1}$$

where ρ is the fluid density, g is the acceleration due to gravity, c_g is the group velocity of the waves, and a is the wave amplitude. The rate of energy dissipation is equal to the time-averaged product of the time-varying bottom shear stress, $\tau_b(t)$, and near-bottom wave orbital velocity, $u_b(t)$.

$$\dot{E}_{diss} = \overline{\tau_b(t) u_b(t)} \tag{2}$$

For sinusoidal waves, $u_b(t) = u_{bm} f(t) = u_{bm} \cos \omega t$, where u_{bm} is the maximum near-bottom orbital velocity and ω is the radian frequency of the waves. The temporal variation of the shear stress is typically taken as related to the square of or linearly related to the temporal variation of the instantaneous near-bottom velocity. Thus, for linear waves,

$$\tau_b(t_\tau) = \tau_{bm} \begin{cases} |f(t_\tau)| f(t_\tau) \\ f(t_\tau) \end{cases} = \frac{1}{2} \rho f_w u_{bm}^2 \begin{cases} |\cos(\omega t + \varphi_\tau)| \cos(\omega t + \varphi_\tau) \\ \cos(\omega t + \varphi_\tau) \end{cases} \tag{3}$$

[1] Graduate student, R. M. Parsons Laboratory, Department of Civil and Environmental Engineering, Massachusetts Institute of Technology, Cambridge, MA 02139, USA. chumbyrd@mit.edu
[2] Donald and Martha Harleman Professor, R. M. Parsons Laboratory, Department of Civil and Environmental Engineering, Massachusetts Institute of Technology, Cambridge, MA 02139, USA. osm@mit.edu

where τ_{bm} is the maximum bottom shear stress, f_w is the wave friction factor, and φ_τ is the phase lead of the shear stress with respect to the near-bottom velocity. Substituting these expressions into Eq. 2 and simplifying gives

$$\dot{E}_{diss} = \begin{Bmatrix} \frac{2}{3\pi} \\ \frac{1}{4} \end{Bmatrix} \rho f_w \cos\varphi_\tau \, u_{bm}^3 = \begin{Bmatrix} \frac{2}{3\pi} \\ \frac{1}{4} \end{Bmatrix} \rho f_e u_{bm}^3, \tag{4}$$

which shows that the energy dissipation factor (also referred to as the energy friction factor) is related to the wave friction factor through a cosine of the phase angle: $f_e = f_w \cos\varphi_\tau$. We choose to take the simple harmonic time variation of the shear stress, corresponding to the second lines of Eq. 3 and 4 with the final factor of 1/4. By simply equating Eq. 1 and 4 the wave energy dissipation factor can be calculated directly from the measured wave height decay.

Common and proposed methods

When ripples cover the bed, the equivalent Nikuradse sand grain roughness, k_n, can be expected to scale with the ripple dimensions. Therefore, the common method of predicting bed roughness begins by predicting the ripple height, η, and possibly the length, λ, and then takes the roughness as a function of these dimensions. It has been shown (e.g., Wikramanayake and Madsen 1994, Styles and Glenn 2002) that the roughness may be well represented as a constant multiple of the ripple height, i.e., $k_n = \alpha\eta$, where α denotes the proportionality constant. The difficulty with the common method thus comes in choosing the appropriate value for α, which is not a physically determined parameter. In fact, the correct value depends on the choice of theoretical friction factor model to be used in further computations and must be determined empirically for each model, e.g., by fitting experimentally observed energy dissipation rates. The chosen theoretical friction factor model is used to back-calculate the roughness from the energy friction factor information, and the best fit α-value is determined by relating the roughness to the measured ripple dimensions. Once α is known for a given model, the roughness is easily predicted from estimates of the ripple dimensions, usually predicted with an empirical relationship.

As the ripple dimensions are not otherwise needed, predicting them is an unnecessary step and may introduce unnecessary error. If the energy friction factor is predicted instead, the roughness can be back-calculated using any desired theoretical friction factor model without the need for a model-dependent constant. Using an empirical relationship for the energy friction factor allows the roughness to be determined entirely from wave, sediment, and fluid information.

Relevant non-dimensional parameters. The two relevant non-dimensional parameters in this boundary layer problem are the skin-friction Shields parameter, ψ', which includes the effects of flow and sediment properties, and the fluid-sediment parameter, S_*, which accounts for the influence of sediment and fluid characteristics. They are given by

$$\psi' = \frac{\frac{1}{2} f_w' u_{bm}^2}{(s-1)gd} \tag{5}$$

and

$$S_* = \frac{d\sqrt{(s-1)gd}}{4\nu} \tag{6}$$

respectively, where the skin-friction factor $f_w' = f_w(k_n' = d)$ is the wave friction factor for a flat sand bed, s is the ratio of sediment to water density ($s = 2.65$ for quartz in freshwater), $d = d_{50}$ is the median sediment grain diameter, and ν is the kinematic viscosity of the fluid.

Theoretical friction factor models. Both methods require a theoretical friction factor model relating the bed roughness to the friction factor. Any friction factor model can be used with either method; we chose to consider two common friction factor models: Jonsson's (1966) model for the wave friction factor and Madsen's (1994) model for the energy friction factor. As stated above, the two friction factors are related by a cosine of the phase angle, which, while sometimes large, is nevertheless often neglected (Wikramanayake and Madsen 1994). The friction factors are given as functions of the relative roughness, A_{bm}/k_n, where A_{bm} is the maximum near-bottom semi-excursion amplitude, related to the orbital velocity by $A_{bm} = u_{bm}/\omega$ for sinusoidal wave motion. Swart (1976) gave an explicit expression for Jonsson's wave friction factor model, denoted by $f_{w,J}$.

$$f_{w,J} = \begin{cases} 0.3, & \dfrac{A_{bm}}{k_n} < \dfrac{1}{0.63} \approx 1.6 \\ \exp\left\{5.213\left(\dfrac{A_{bm}}{k_n}\right)^{-0.194} - 5.977\right\}, & \dfrac{A_{bm}}{k_n} \geq \dfrac{1}{0.63} \approx 1.6 \end{cases} \quad (7)$$

Madsen's model for the energy friction factor, given by $f_{e,M} = f_{w,M}\cos\varphi_{\tau,M}$, can be expressed in a similar explicit form following Swart (1976).

$$f_{w,M} = \begin{cases} \exp\left\{7.02\left(\dfrac{A_{bm}}{k_n}\right)^{-0.078} - 8.82\right\}, & 0.2 < \dfrac{A_{bm}}{k_n} \leq 10^2 \\ \exp\left\{5.61\left(\dfrac{A_{bm}}{k_n}\right)^{-0.109} - 7.30\right\}, & 10^2 < \dfrac{A_{bm}}{k_n} \leq 10^4 \end{cases} \quad (8)$$

$$\varphi_{\tau,M} = \frac{\pi}{60}\left[11 - 2.0\log_{10}\left(\frac{A_{bm}}{k_n}\right)\right], \qquad 0.2 < \frac{A_{bm}}{k_n} \leq 10^3$$

The friction factor models give quite different results for large roughnesses (small values of A_{bm}/k_n, e.g., in the ripple regime), while for very small roughnesses (large values of A_{bm}/k_n) they give nearly identical values (Figure 1). At the small A_{bm}/k_n end, for example, for a typical friction factor value of 0.2, the Madsen and Jonsson models give $A_{bm}/k_n = 0.5$ and 2.5, respectively, a factor of 5 difference. The skin-friction factor is found at the other end, corresponding to very large A_{bm}/k_n values, as it is calculated for a flat sand bed, i.e., $f_w' = f_w(A_{bm}/k_n' = A_{bm}/d)$, and over the typical range of A_{bm}/d values the models differ on average by less than 10%. It follows that the skin-friction Shields parameter is fairly insensitive to the choice of friction factor theory.

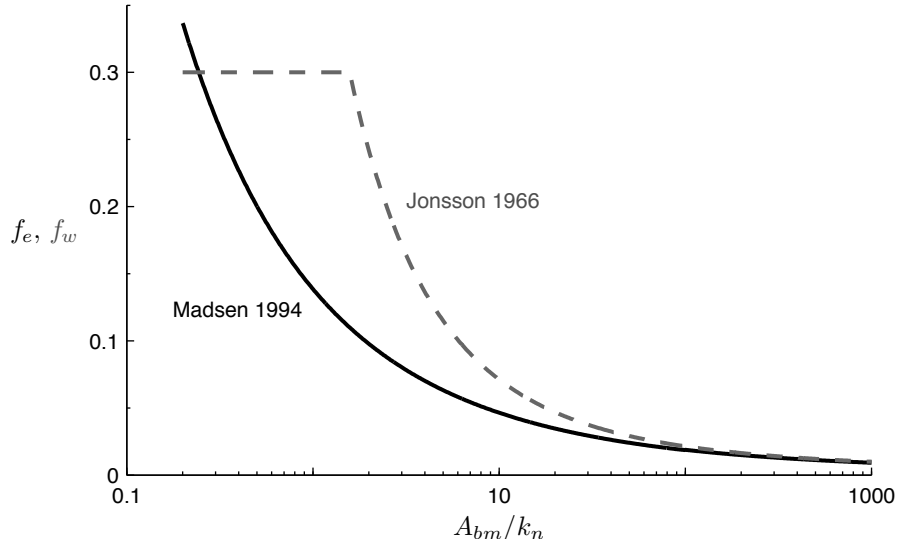

Figure 1. Theoretical friction factor models of Madsen (1994) and Jonsson (1966)

MOVABLE BED ROUGHNESS FROM THE LABORATORY

Common method

The common method requires a prediction of ripple geometry and there is no lack of published empirical relationships from laboratory and field measurements relating ripple dimensions to flow and sediment characteristics (e.g., Miller and Komar 1980, Nielsen 1981, Grant and Madsen 1982, Kos'yan 1988, Wikramanayake and Madsen 1994, Wiberg and Harris 1994, Mogridge et al. 1994, Faraci and Foti 2002, Williams et al. 2004, O'Donoghue et al. 2006). Each formula performs well against the data used in its formulation, as expected, but generally much less successfully under reasonably different conditions. Thus, instead of choosing a published relationship, we developed our own from all of the laboratory data we could acquire, including most of the data used to develop those expressions.

Some researchers (e.g., Nielsen 1981, Wikramanayake and Madsen 1994, Kos'yan 1988) have concluded that ripple geometry relationships developed from laboratory data are not applicable to field conditions. However, these conclusions were formed after comparing relatively small-scale laboratory data under periodic waves to field data and did not consider laboratory data on random waves. We

chose not to include field data of ripple dimensions because all of the available data on energy dissipation are from small-scale laboratory experiments. Since the energy dissipation data are needed to find the α-value in the common method and the expression for the energy friction factor in the proposed method, by using laboratory data exclusively we ensure that we are both consistent within the development of this method and when comparing the two methods.

Several movable bed data sets from laboratory experiments with periodic and random waves (Table 1) were analyzed to obtain a relationship for the ripple height. Only a ripple height relationship is required since we choose to take the roughness as a constant multiple of the ripple height. The ripple height is scaled by the maximum near-bottom semi-excursion amplitude, A_{bm}. For sinusoidal wave motion, as stated above, $A_{bm} = u_{bm}/\omega$. For random waves, the corresponding wave parameters are found by defining a representative periodic wave that is equivalent to the random wave spectrum. Madsen (1994) showed that the near-bottom orbital velocity amplitude of the representative periodic wave is the root-mean-square (rms) velocity amplitude, $u_{b,rms}$, and the representative radian frequency, ω_r, is the mean frequency of the spectrum (given explicitly in the Appendix). Thus, for random waves, the maximum near-bottom semi-excursion amplitude is defined as $A_{bm,random} = u_{b,rms}/\omega_r$.

Table 1. Overview of laboratory datasets used in ripple height analysis

Flow type	No. datasets	No. data points	No. diameters	d (mm)	ψ' [(a)]	η/A_{bm}
Periodic waves	17	473	23	0.082-0.585	0.02-1.47	0-0.50
Random waves	6	90	9	0.12 -0.56	0.05-1.02	0-0.36

Note: Full references provided in REFERENCES section, identified by '*'

[a] Calculated with the significant near-bottom orbital velocity for random waves (Eq. 9)

We found that the skin-friction Shields parameter effectively correlated the non-dimensional ripple height, η/A_{bm}; however, the data were still stratified according to sediment size, with the larger diameters creating larger ripples for the same value of the Shields parameter. O'Donoghue et al. (2006) noticed a similar trend in their field-scale experiments. They classified the ripples as either 2D or 3D; the 2D ripples nearly always corresponded to diameters of 0.30 mm or larger while the 3D ripples were only found with diameters of 0.22 mm or smaller. The dimensions of the 3D ripples, from the smaller sands, were reasonably well represented as a constant fraction of the 2D ripple dimensions, given by multiplying the empirical 2D-ripple fit by a factor smaller than one (e.g., 0.55 for the ripple height prediction). While our data showed a distinct stratification according to sediment size, we did not have information on the bedform type for all of the experiments, so we cannot comment on whether the stratification is related to different ripple patterns. Van Rijn (2007) claims that bed roughness is proportional to sediment diameter for sediments smaller than 0.5 mm; since he took the roughness as proportional to ripple height, it follows that ripple height is also proportional to sediment size. Similar to van Rijn, we did not see a clear division between the ripple heights for sediments above or below a certain size as O'Donoghue et al. did, rather we saw a gradual decrease in ripple height with decreasing sediment diameter. In light of this continuous variation, we included a factor of $S_*^{-0.25}$, with the power found by a least squares fitting to the data, with the non-dimensional ripple height to lessen the sediment size stratification. While including an S_* factor worked well with these data, whether it is the optimal method to destratify the data is unknown; however, there does appear to be consensus that overall, ripple height, and thus bed roughness, increases with sediment size.

While the ripples under periodic and random waves follow the same general trend and show the same S_* stratification, the ripples under random waves decay much faster as the Shields parameter increases. The flat-bed (sheet-flow) state is reached under random waves at about $\psi' = 0.4$, while the ripples under periodic waves do not disappear until $\psi' = 0.8$, suggesting a difference in the skin-friction Shields parameter of order 2. This difference is seen when the rms near-bottom orbital velocity is used in the Shields parameter for the random waves, that is, $\psi'_{random} = \psi'_{rms} = \psi'(u_{bm} = u_{b,rms})$. However, if the significant (sig) near-bottom velocity is used for the random waves, i.e., $\psi'_{random} = \psi'\left(u_{bm} = u_{b,sig} = \sqrt{2}u_{b,rms}\right) = 2\psi'_{rms}$, the Shields parameter is doubled and the transition to flat-bed occurs around $\psi' = 0.8$ for both wave conditions. It is physically reasonable to expect the larger waves in a random wave train to have a greater effect on the ripple dimensions than the smaller waves, which suggests that a near-bottom velocity greater than the rms velocity is necessary to represent random waves. Faraci and Foti (2002) and Williams et al. (2004) similarly found that a single relationship could be used to represent ripple geometry under both types of waves if the significant wave height was used for the random waves. Furthermore, representing random waves with the significant near-bottom velocity has been used to successfully consolidate data in other boundary layer processes, such as

initiation of motion (Madsen 2002). O'Donoghue et al. (2006) found that using the mean of the highest 1/10 near-bottom velocities for the random waves (hereafter referred to as the 1/10 velocity) more effectively merged their periodic and random wave data than using the significant velocity; however, using the 1/10 velocity gave a worse fit for our data. It should be noted that the difference between the fits found using the significant and 1/10 near-bottom velocity is minimal since the random-wave data make up only 16% of the full data set. We have therefore decided to use the significant near-bottom velocity in the skin-friction Shields parameter for the random waves as this consolidates the transition to flat bed and gives a better overall fit to our data. By defining the skin-friction Shields parameter as

$$\psi' = \frac{\frac{1}{2}f_w'}{(s-1)gd} \cdot \begin{cases} u_{bm}^2, & \text{for periodic waves} \\ \left(\sqrt{2}u_{b,rms}\right)^2, & \text{for random waves} \end{cases} \qquad (9)$$

a single relationship can be found that well represents ripple heights under both types of waves:

$$\frac{\eta}{A_{bm}} = 0.16 S_*^{0.25} \exp\{-2.67\psi'\} \qquad (10)$$

This equation, found by a least squares fitting, does a reasonable job representing both the periodic and random wave data, despite the inherent scatter: 79% of the data lie within ±50% of the best fit line, and the RMS-error of predicting the non-dimensional ripple height with Eq. 10 is 0.05 (Figure 2).

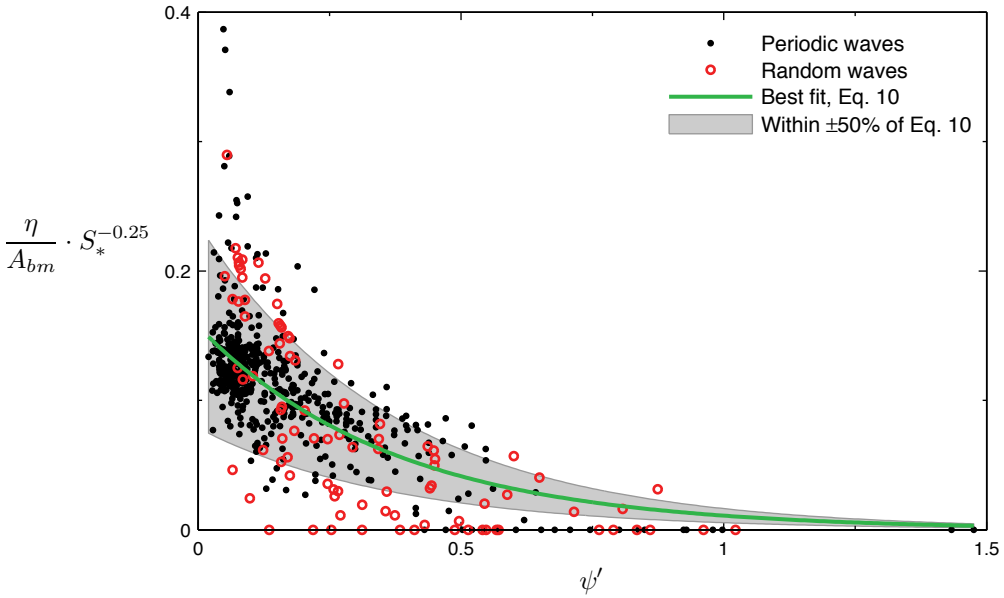

Figure 2. Periodic and random wave laboratory data and least squares fit of the non-dimensional ripple height as a function of the skin-friction Shields parameter and fluid-sediment parameter

Once the ripple dimensions are predicted, the roughness can be easily estimated as a function of those dimensions. We choose to take the roughness as $k_n = \alpha\eta$, but, as mentioned above, α varies with the choice of theoretical friction factor model and is determined from observed energy dissipation rates. Laboratory data of energy dissipation under both periodic and random waves over movable beds (Table 2) were used to determine α for the chosen theoretical friction factor models. The best-fit α-value was found to be 8 when the Madsen (1994) model is used, but it is 2 for the Jonsson (1966) model. The variability in α is a major shortcoming of the common method. Even if the ripple dimensions are predicted perfectly, the accuracy of the roughness prediction is nevertheless tied to the precision of this constant, which in turn relies wholly on the energy friction factor data.

Table 2. Overview of laboratory datasets used in energy dissipation analysis

Flow type	No. datasets	No. data points	No. diameters	d (mm)	ψ' [(a)]	f_e
Periodic waves	4	145	7	0.12-0.585	0.02-0.62	0.06-0.47
Random waves	2	26	2	0.12-0.20	0.06-0.19	0.05-0.40

Note: Full references provided in REFERENCES section, identified by '†'

[a] Calculated with the significant near-bottom orbital velocity for random waves (Eq. 9)

Proposed method

Using the same energy dissipation data that were used to determine the α-values for the common method (Table 2), we instead found a relationship to directly predict the energy dissipation factor from fluid, flow, and sediment characteristics. As in the case of ripple height, we found that the energy friction factor correlates well with the skin-friction Shields parameter, using, as before, the significant near-bottom velocity in the Shields parameter for the random wave data. The energy friction factor data were also stratified according to their S_* values, so we again included the factor of $S_*^{-0.25}$ to consolidate the different sediment sizes, where the best-fit power of S_* happened to be the same as for the ripple height analysis. Using the definition of the skin-friction Shields parameter given by Eq. 9, the energy friction factor can be predicted with Eq. 11, which was found by a least squares fit to the data.

$$f_e = 0.14 S_*^{0.25} \exp\{-2.47\psi'\} \qquad (11)$$

This expression for the energy dissipation factor was developed solely from measurements over rippled beds and therefore is only applicable to the ripple regime, i.e., for $\psi' < 0.8$. Eq. 11 fits the data well: 73% of the data are contained within ±25% of the best fit line and the RMS-error of predicting the energy dissipation factor is 0.05 (Figure 3).

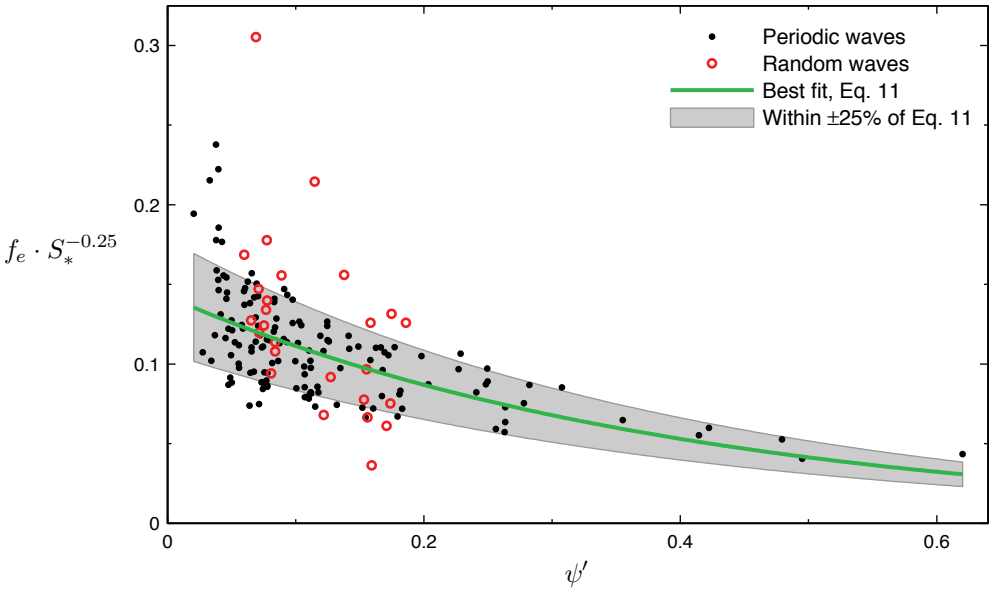

Figure 3. Periodic and random wave laboratory data and least squares fit of the energy dissipation factor as a function of the skin-friction Shields parameter and fluid-sediment parameter

Once the energy friction factor is predicted using this expression, the bed roughness can be back-calculated using any preferred friction factor model, such as Eq. 7 or 8. No model-dependent constant is required for this method.

APPLICATION TO FIELD CONDITIONS

It is ultimately of interest to predict transport in the field, not the lab, and the methods are therefore rather useless if they do not perform well for field conditions. The methods were developed entirely with laboratory data, and there is no reason to believe that the relationships are applicable to field scale. Indeed, previous ripple geometry relations have yielded poor results when applied to field data, and it seems reasonable that the α-value and energy dissipation rate could likewise be different under field conditions. Nevertheless, since the expressions would be used to make predictions in the field, it is prudent to evaluate the methods with field data.

Since both waves and currents, to varying degrees, are typically found together in the field, a wave-current model must be applied to make predictions under these conditions. After the roughness is calculated using either method from measured wave and sediment information, a wave-current model can be applied with measured wave, sediment, and current information, along with the predicted bed roughness, to predict the current velocity profile. Note that the choice of wave-current model should be consistent with the friction factor model used to determine the α-value for the common method or used to calculate the roughness for the proposed method.

Both methods were tested with three data sets of current profiles in combined wave-current flows over rippled beds in the field (Table 3), yielding a total of 74 current velocities 100 cm above the bottom (cmab). When the current velocity was not measured at 100 cmab, it was calculated using the shear velocity and apparent roughness determined by the authors from the current profiles. These observed velocities were compared with the predictions afforded by Madsen's (1994) modified wave-current model (summarized in the Appendix) using the roughness relationships derived from lab data, together with measured wave and sediment characteristics, and specifying the current in terms of its direction relative to the waves and its shear velocity. As waves in the field are certainly random, the significant near-bottom velocity was used to calculate the skin-friction Shields parameter for the roughness relationships. When applied to random waves, the Madsen (1994) modified wave-current model requires the rms near-bottom orbital velocity.

Table 3. Overview of wave-current field datasets used to evaluate methods

Source	No. data points	Water depth (m)	d (mm)	ω (s^{-1})	ψ' [a]
Styles and Glenn (2002)	47	12	0.4	0.53-0.88	0.04 -0.12
Xu and Wright (1995)[b]	4	14	0.12	0.55-0.86	0.30 -0.48
Drake et al. (1992)	23	35	0.25	0.45-1.21	0.004-0.02

Note: Full references provided in REFERENCES section, identified by '‡'
[a] Calculated with the significant near-bottom orbital velocity
[b] Subset only: the 4 experiments of sheet flow during the Halloween storm of 1991 were excluded

For the common method, the ripple height was predicted with Eq. 10 and the bottom roughness was taken as 8 times the height, where $\alpha = 8$ is the best-fit factor for Madsen's (1994) model. The common method does a reasonable job predicting the field data: the predictions are biased by a factor of 0.94±0.23 and the RMS-error is 3.9 cm/s (Figure 4, left panel). The bias is taken as the average slope of the data points, that is, the average of the ratio of the predicted over the measured current velocities, equal to 0.94 in this case, and is given as plus or minus one standard deviation, 0.23 here, corresponding to an underprediction of 6±23%. With this definition, the line of the average slope can be expressed as $u_{c,pred} = 0.94u_{c,meas}$, where u_c is the current velocity and the subscripts *pred* and *meas* refer to the predicted and measured values, respectively.

For the proposed alternative method, the energy dissipation factor was predicted with Eq. 11 and Madsen's (1994) energy friction factor relationship, Eq. 8, was used to calculate the bed roughness. This approach predicts the current as well as the common method, giving a slightly larger but more tightly bounded bias of 0.92±0.21 and a RMS-error of only 3.1 cm/s (Figure 4, right panel).

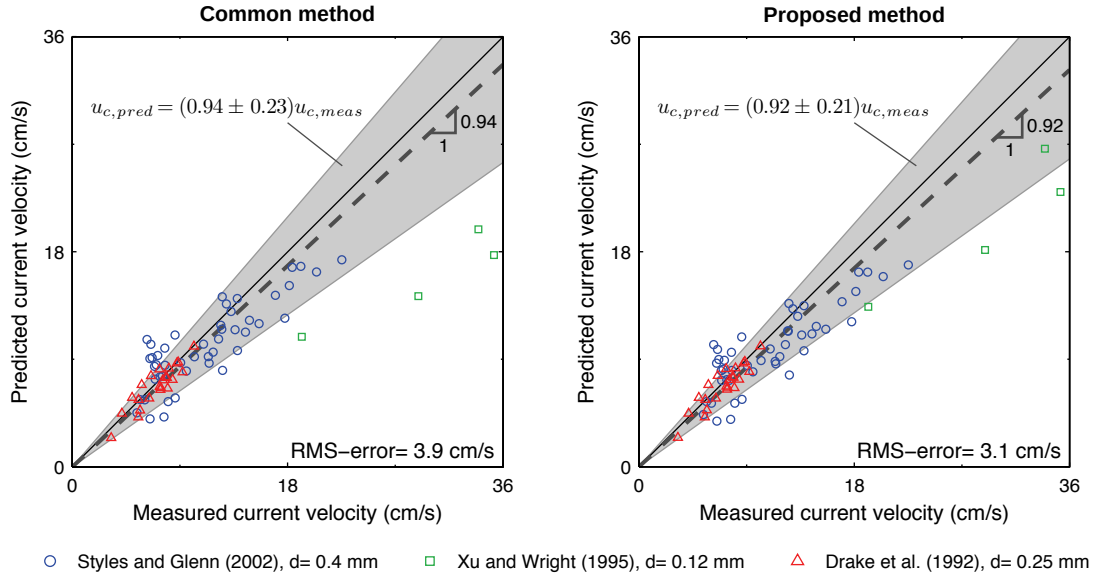

Figure 4. Comparison between predicted and measured current velocities 100 cmab. The solid line denotes perfect agreement while the dashed line shows the average slope of the data points and the gray band covers ±1 standard deviation of the average slope, corresponding to an underprediction of 6±23% and 8±21%, respectively, for the common (left panel) and proposed (right panel) methods.

Both methods underpredict the current velocity by about 7% on average (Figure 4), resulting from an overprediction of the bed roughness. To predict a smaller, and presumably more correct, roughness, a larger value of the Shields parameter is required, which corresponds to a larger near-bottom velocity. This is true for both methods: for the common method, a larger Shields parameter predicts a smaller ripple height (Figure 2 or Eq. 10) and by $k_n = \alpha\eta$ a smaller roughness; for the proposed method, a larger Shields parameter predicts a smaller energy friction factor (Figure 3 or Eq. 11), which in turn gives a larger value of A_b/k_n (Figure 1 or Eq. 8), or a smaller roughness. As mentioned above, O'Donoghue et al. (2006) had success consolidating data from periodic and random waves by using the mean of the 1/10 highest near-bottom velocities for the random waves. Li and Amos (1999) found that the onset of sheet flow under combined wave-current flow in the field was well represented by the expression for waves alone (developed from mostly lab data) if the significant near-bottom velocity was used for the wave alone data and the 1/10 velocity was used for the combined wave-current data. Drake and Cacchione (1992) compared the predictions of a wave-current model using both the significant and 1/10 near-bottom velocities to describe their field data and found that while the current velocity profile was well predicted during non-storm conditions using either velocity, using the 1/10 near-bottom velocity gave better predictions of the current velocity and sediment response during storm periods. In light of this evidence that the 1/10 near-bottom velocity may better characterize wave-current field flows, we also tested the methods using this larger velocity in the Shields parameter to predict the roughness. Assuming the waves are Rayleigh distributed, the 1/10 velocity is related to the rms velocity by $u_{b,1/10} = 1.8u_{b,rms}$, whereas the significant velocity, used in Figure 4, is related by $u_{b,sig} = \sqrt{2}u_{b,rms}$. Using the 1/10 velocity greatly improves the predictions of both methods: the common method underpredicts the velocities by 3±23% and gives a RMS-error of 3.3 cm/s; the proposed method underpredicts the velocities by 2±21% and gives a RMS-error of only 2.2 cm/s (Figure 5). Note that the 1/10 near-bottom velocity was used in the roughness prediction (Eq. 10 or 11), but the Madsen (1994) modified wave-current model requires the rms velocity.

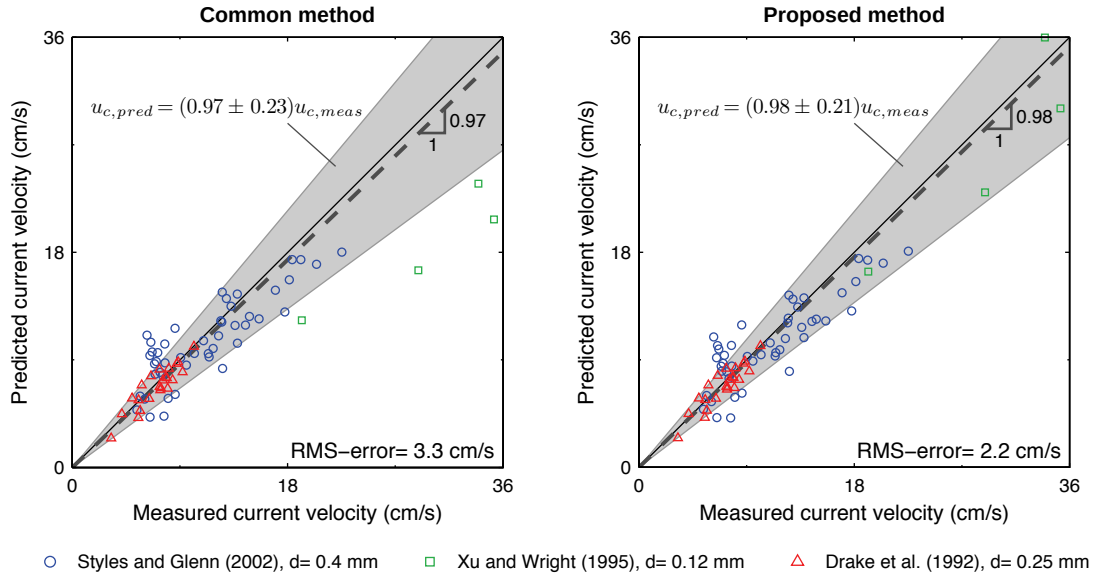

Figure 5. Comparison between predicted and measured current velocities 100 cmab using the 1/10 near-bottom velocity in the Shields parameter. The solid line denotes perfect agreement while the dashed line shows the average slope and the gray band covers ±1 standard deviation of the slope, corresponding to an underprediction of 3±23% and 2±21%, respectively, for the common and proposed methods.

Although the 1/10 near-bottom velocity was used for the field data with success in Figure 5, the roughness was still calculated with the equations developed using the significant near-bottom velocity for the random wave laboratory data. Clearly, to be consistent the same near-bottom velocity should be used in both cases, but the laboratory relationships were tested during development with the 1/10 velocity and gave worse fits. Also, as mentioned previously, there are so few data under random waves relative to periodic waves that the fits found using the significant and 1/10 velocity are quite similar. While the 1/10 velocity gives better results for this limited set of field data, much more field data are required before any conclusion can be made about the appropriate near-bottom velocity for these flows.

CONCLUSION

We have proposed a new method of predicting movable bed roughness in the ripple regime which, unlike the common method, does not include any model dependent factors. This paper outlined the development of both methods with laboratory data and described the initial testing of the methods with combined wave-current field data.

From analyzing an extensive set of laboratory data, we found that both the non-dimensional ripple height and wave energy dissipation factor are well represented as functions of the skin-friction Shields parameter, ψ', and the fluid-sediment parameter, S_*. The data from periodic and random waves correlate well when the significant near-bottom velocity is used in the skin-friction Shields parameter for the random waves. The best fit exponential equations (Eq. 10 and 11) represent the data well: 79% of the non-dimensional ripple height data lie within ±50% of the best-fit line and 73% of the energy dissipation factor data lie within ±25% of the best-fit line. With the roughness taken as $k_n = \alpha\eta$ for the common method, the best-fit α factor is found, using the energy dissipation data, to be equal to 8 and 2 for the Madsen and Jonsson friction factor models, respectively; the wide variability in this factor is a major drawback of this method. The proposed method does not require a model-dependent factor.

There is evidence that ripple geometry relationships derived from laboratory data do not well represent field conditions. We chose not to include field data on ripple dimensions because energy dissipation, used to find the model-dependent α-value in the common method and at the core of the proposed method, can only be reliably measured in the lab. However, while the appropriateness of applying our laboratory-developed equations to field conditions is questionable, we have shown that they provide reasonable predictions of the current velocity in combined wave-current flows in the field.

Both methods yield acceptable accuracy when applied to combined wave-current field data. When the significant near-bottom orbital velocity is used in the skin-friction Shields parameter to predict the roughness of the field flows, the common and proposed methods underpredict the current velocity by 6% and 8% on average and give RMS-errors of 3.9 and 3.1 cm/s, respectively. Better predictions are obtained when the 1/10 near-bottom orbital velocity is used: the underprediction is reduced to 3% and 2% and the RMS-errors decrease to 3.3 and 2.2 cm/s, respectively. More field data will need to be considered before the appropriate representative near-bottom orbital velocity can be determined.

ACKNOWLEDGMENTS

The authors gratefully acknowledge the financial support of the National Research Foundation of Singapore (NRF) through the Singapore-MIT Alliance for Research and Technology's (SMART) Center for Environmental Sensing and Modelling (CENSAM) program.

APPENDIX

Following Madsen (1994), the maximum bed shear stress due to the waves is

$$\tau_{wm} = \frac{1}{2}\rho f_{cw} u_{bm}^2 = \rho u_{*wm}^2 \qquad \text{(A-1)}$$

where u_{*wm} is the maximum wave shear velocity and f_{cw} is the combined wave-current friction factor,

$$f_{cw} = \begin{cases} C_\mu \exp\left\{7.02\left(C_\mu \dfrac{A_{bm}}{k_n}\right)^{-0.078} - 8.82\right\}, & 0.2 < C_\mu \dfrac{A_{bm}}{k_n} \le 10^2 \\ C_\mu \exp\left\{5.61\left(C_\mu \dfrac{A_{bm}}{k_n}\right)^{-0.109} - 7.30\right\}, & 10^2 < C_\mu \dfrac{A_{bm}}{k_n} \le 10^4 \end{cases} \qquad \text{(A-2)}$$

with

$$C_\mu = \sqrt{1 + 2|\cos\phi_{cw}|\mu + \mu^2} \qquad \text{(A-3)}$$

where

$$\mu = \frac{\tau_c}{\tau_{wm}} = \frac{u_{*c}^2}{u_{*wm}^2}, \qquad \text{(A-4)}$$

ϕ_{cw} is the angle between the current and the direction of wave propagation, and τ_c is the bed shear stress due to the current, related to the current shear velocity, u_{*c}, by $\tau_c = \rho u_{*c}^2$.

The current velocity at a height z_r above the bed, $u_{c,r} = u_c(z = z_r)$, is given by

$$u_{c,r} = \begin{cases} \dfrac{u_{*c}^2}{\kappa u_{*m}} \ln \dfrac{z_r}{z_0}, & z < \delta_{wc} \\ \dfrac{u_{*c}}{\kappa} \ln \dfrac{z_r}{z_{0a}}, & z \geq \delta_{wc} \end{cases} \quad \text{(A-5)}$$

where $\kappa = 0.4$, $30z_0 = k_n$, $30z_{0a} = k_{na}$, where k_{na} is the apparent roughness and

$$z_{0a} = z_0 \left(\frac{\delta_{cw}}{z_0}\right)^{1-\frac{u_{*c}}{u_{*m}}}, \quad \text{(A-6)}$$

u_{*m} is the wave-current shear velocity given by $u_{*m}^2 = C_\mu u_{*wm}^2$, and the transition between the two log-linear profiles occurs at $z = \delta_{wc}$, given by

$$\delta_{wc} = \frac{\kappa u_{*m}}{\omega} \left(\frac{C_\mu}{\mu}\right)^{\frac{1}{2}\frac{\sqrt{C_\mu}}{\sqrt{C_\mu}-\sqrt{\mu}}} \frac{1}{16.3} \exp\left\{2.96\left(C_\mu \frac{A_{bm}}{k_n}\right)^{-0.071} - 1.45\right\}. \quad \text{(A-7)}$$

To apply the model to random waves, the near-bottom parameters of the representative periodic wave, which is equivalent to the spectral wave representation, are used: $u_{bm} = u_{b,rms}$ and $A_{bm} = u_{b,rms}/\omega_r$, where ω_r is the mean radian frequency, obtained from the random wave spectrum by

$$\omega_r = \frac{\int \omega S_\eta(\omega) d\omega}{\int S_\eta(\omega) d\omega}. \quad \text{(A-8)}$$

For the wave-current analysis in this paper, the values of $u_{b,rms}$ and ω_r for the waves, u_{*c} for the current, and ϕ_{cw} were provided in the field datasets. The bottom roughness was predicted with the specified wave and sediment information using either of the two methods outlined. We initially set $C_\mu = 1$ and calculate the friction factor, maximum bed shear stress, and the updated values of μ and C_μ using Eq. A-2, A-1, A-4, and A-3, respectively, and iterate until C_μ converges. The current velocity profile is then calculated by Eq. A-5 with the unknown values evaluated explicitly by Eq. A-6 and A-7.

REFERENCES

*†Carstens, M.R., F.M. Nielson, and H.D. Altinbilek. 1969. *Bed Forms Generated in the Laboratory Under an Oscillatory Flow: Analytical and Experimental Study*, U.S. Army Corps of Engineers, Coastal Engineering Research Center, TM-28, Vicksburg, MS.

Drake, D.E., and D.A. Cacchione. 1992. Wave-current interaction in the bottom boundary layer during storm and non-storm conditions: observations and model predictions, *Continental Shelf Research*, 12, 1331-1352.

‡Drake, D.E., D.A. Cacchione, and W.D. Grant. 1992. Shear stress and bed roughness estimates for combined wave and current flows over a rippled bed, *Journal of Geophysical Research*, 97, 2319-2326.

Faraci, C., and E. Foti. 2002. Geometry, migration and evolution of small-scale bedforms generated by regular and irregular waves, *Coastal Engineering*, 35-52.

Grant, W. D., and O.S. Madsen. 1982. Movable bed roughness in unsteady oscillatory flow, *Journal of Geophysical Research*, 87, 469-481.

*Inman, D. L., and A.J. Bowen. 1963. Flume experiments on sand transport by waves and currents, *Proceedings of the 8th Coastal Engineering Conference*, 137-150.

Jonsson, I.G. 1966. Wave boundary layers and friction factors, *Proceedings of 10th Conference on Coastal Engineering,* 127-148.

*Kennedy, J. F., and M. Falcon. 1965. *Wave Generated Sediment Ripples*, Hydrodynamics Laboratory, Dept. of Civil Engineering, Massachusetts Institute of Technology, Report 86, Cambridge, MA.

Kos'yan, R.D. 1988. On the dimensions of passive ripple marks in the nearshore zone, *Marine Geology*, 80, 149-153.

*Lambie, J. M. 1984. *An Experimental Study of the Stability of Oscillatory Flow Bed Configurations*, M.S. thesis, Massachusetts Institute of Technology, Cambridge, MA.

Li, M.Z., and C.L. Amos. 1999. Sheet flow and large wave ripples under combined waves and currents: field observations, model predictions and effects on boundary layer dynamics, *Continental Shelf Research*, 19, 637-663.

*Lofquist, K.E.B. 1978. *Sand Ripple Growth in an Oscillatory-Flow Water Tunnel*. U.S. Army Corps of Engineers, Coastal Engineering Research Center, TP-78-5, Fort Belvoir, VA.

*†Lofquist, K.E.B. 1986. *Drag on Naturally Rippled Beds Under Oscillatory Flows*, U.S. Army Corps of Engineers, Coastal Engineering Research Center, MP-86-13, Vicksburg, MS.

Madsen, O.S. 1994. Spectral wave-current bottom boundary layer flows. *Proceedings of 24th International Conference on Coastal Engineering,* ASCE, 384-398.

Madsen, O.S. 2002. Sediment Transport Outside the Surf Zone. In: Walton, T. (editor), *Coastal Engineering Manual*, Part III, Coastal Processes, Chapter III-6, Engineer Manual 1110-2-1100, U.S. Army Corps of Engineers, Washington, DC.

*†Mathisen, P.P. 1989. *Experimental Study on the Response of Fine Sediments to Wave Agitation and Associated Wave Attenuation*, M.S. thesis, Massachusetts Institute of Technology, Cambridge, MA.

*Miller, M.C., and P.D. Komar. 1980. Oscillation sand ripples generated by laboratory apparatus, *SEPM Journal of Sedimentary Research*, 50.

*Mogridge, G. R., and J.V. Kamphuis. 1972. Experiments on bed form generation by wave action, *Proceedings of the 13th Coastal Engineering Conference*, 1123-1142.

Mogridge, G., M. Davies, and D. Willis. 1994. Geometry prediction for wave-generated bedforms, *Coastal Engineering*, 255-286.

*Nielsen, P. 1979. *Some Basic Concepts of Wave Sediment Transport*, Series Paper No. 20, Institute of Hydrodynamics and Hydraulic Engineering, Technical University of Denmark.

Nielsen, P. 1981. Dynamics and geometry of wave-generated ripples, *Journal of Geophysical Research*, 86, 6467-6472.

*O'Donoghue, T., and G.S. Clubb. 2001. Sand ripples generated by regular oscillatory flow, *Coastal Engineering*, 44, 101-115.

*O'Donoghue, T., J.S. Doucette, J.J. van der Werf, and J.S. Ribberink. 2006. The dimensions of sand ripples in full-scale oscillatory flows, *Coastal Engineering,* 53, 997-1012.

*Ribberink, J. S., and A.A. Al-Salem. 1994. Sediment transport in oscillatory boundary layers in cases of rippled beds and sheet flow, *Journal of Geophysical Research*, 99, 12707-12727.

*†Rosengaus, M. 1988. *Experimental Study on Wave Generated Bedforms and Resulting Wave Attenuation*, Ph.D. thesis, Massachusetts Institute of Technology, Cambridge, MA.

*Sato, S. 1987. *Oscillatory Boundary Flow and Sand Movement Over Ripples*, Ph.D. thesis, University of Tokyo, Tokyo, Japan.

*Sato, S., and K. Horikawa. 1988. Sand ripple geometry and sand transport mechanism due to irregular oscillatory flows, *Proceedings of the 21st Coastal Engineering Conference*, 1748-1762.

‡Styles, R., and S.M. Glenn. 2002. Modeling bottom roughness in the presence of wave-generated ripples, *Journal of Geophysical Research*, 107, 24/1-24/15.

Swart, D.H. 1976. Predictive equations regarding coastal transports, *Proceedings of 15th Conference on Coastal Engineering*, 2:1113-1132.

*Thorne, P. D., A.G. Davies, and J.J. Williams. 2003. Measurements of near-bed intra-wave sediment entrainment above vortex ripples, *Geophysical Research Letters*, 30, 4 pp.

*Thorne, P. D., J.J. Williams, and A.G. Davies. 2002. Suspended sediments under waves measured in a large-scale flume facility, *Journal of Geophysical Research*, 107, 16 pp.

*van der Werf, J.J., J.J.L.M. Schretlen, J.S. Ribberink, and T. O'Donoghue. 2009. Database of full-scale laboratory experiments on wave-driven sand transport processes, *Coastal Engineering,* 56, 726-732.

*van der Werf, J.J., J.S. Doucette, T. O'Donoghue, and J.S. Ribberink. 2007. Detailed measurements of velocities and suspended sand concentrations over full-scale ripples in regular oscillatory flow, *Journal of Geophysical Research*, 112, 18 pp.

van Rijn, L.C. 2007. Unified view of sediment transport by currents and waves. I: Initiation of motion, bed roughness, and bed-load transport, *Journal of Hydraulic Engineering*, 133, 649-667.

Wiberg, P.L., and C.K. Harris. 1994. Ripple geometry in wave-dominated environments, *Journal of Geophysical Research*, 99, 775-789.

Williams, J.J., P.S. Bell, P.D. Thorne, N. Metje, and L.E. Coates. 2004. Measurement and prediction of wave-generated suborbital ripples, *Journal of Geophysical Research*, 109, 18 pp.

Wikramanayake, P.N., and O.S. Madsen. 1994. *Calculation of Movable Bed Friction Factors*, U.S. Army Engineer Waterways Experiment Station, DRP-94-5, Vicksburg, MS.

‡Xu, J.P., and L.D. Wright. 1995. Tests of bed roughness models using field data from the Middle Atlantic Bight, *Continental Shelf Research,* 15, 1409-1434.

---

* Laboratory data used in ripple geometry analysis (Table 1)

† Laboratory data used in energy dissipation analysis (Table 2)

‡ Wave-current field data (Table 3)